

SPECTRAL RESOLUTION-LINKED BIAS IN TRANSIT SPECTROSCOPY OF EXTRASOLAR PLANETS

DRAKE DEMING^{1,2} AND KYLE SHEPPARD¹
Draft version June 23, 2021

ABSTRACT

We re-visit the principles of transmission spectroscopy for transiting extrasolar planets, focusing on the overlap between the planetary spectrum and the illuminating stellar spectrum. Virtually all current models of exoplanetary transmission spectra utilize an approximation that is inaccurate when the spectrum of the illuminating star has a complex line structure, such as molecular bands in M-dwarf spectra. In those cases, it is desirable to model the observations using a coupled stellar-planetary radiative transfer model calculated at high spectral resolving power, followed by convolution to the observed resolution. Not consistently accounting for overlap of stellar M-dwarf and planetary lines at high spectral resolution can bias the modeled amplitude of the exoplanetary transmission spectrum, producing modeled absorption that is too strong. We illustrate this bias using the exoplanet TRAPPIST-1b, as observed using HST/WFC3. The bias in this case is about 250 parts-per-million, 12% of the modeled transit absorption. Transit spectroscopy using JWST will have access to longer wavelengths where the water bands are intrinsically stronger, and the observed signal-to-noise ratios will be higher than currently possible. We therefore expect that this resolution-linked bias will be especially important for future JWST observations of TESS-discovered super-Earths and mini-Neptunes transiting M-dwarfs.

Subject headings: planets and satellites: atmospheres - techniques: spectroscopic - radiative transfer

1. INTRODUCTION

Transit spectroscopy is a productive method to derive the atmospheric properties of transiting extrasolar planets. The first successful transit spectroscopy exploited strong atomic lines to probe the exoplanetary atmosphere (e.g., Charbonneau et al. 2002; Redfield et al. 2008). In the past few years, the WFC3 instrument on the Hubble Space Telescope has been used to measure water vapor absorption at 1.4 μm in giant planets (Deming et al. 2013; Kreidberg et al. 2014a; Fraine et al. 2014; Nikolov et al. 2015; Evans et al. 2016; Sing et al. 2016), and provide stringent upper limits for smaller planets (Kreidberg et al. 2014b; Knutson et al. 2014).

A future goal of transit spectroscopy is to measure molecular absorption in the atmosphere of a habitable super-Earth transiting a nearby M-dwarf star, e.g. using JWST (Deming et al. 2009; Cowan et al. 2015). The TESS mission (Ricker et al. 2015) will discover the best systems for this quest, but already the ground-based surveys are finding excellent candidates such as GJ1132b (Berta-Thompson et al. 2015), TRAPPIST-1 (Gillon et al. 2016; de Wit et al. 2016; Barstow & Irwin 2016; Gillon et al. 2017), and even a (non-transiting) planet orbiting Proxima Centauri (Anglada-Escude et al. 2016). Considering the increasing attention paid to planets that orbit M-dwarf stars, and the imminent plans for JWST observations (Stevenson et al. 2016; Greene et al. 2016), factors that affect transit spectroscopy of such planets are of urgent interest.

In this *Letter* we describe an important effect that is relevant to transit spectroscopy of planets transiting M-dwarf stars. In brief, the line absorption spectrum of the host star can bias the inferred transit spectrum of the planet. The bias is not in the observations per se, it occurs when

modeling of the transit spectrum utilizes insufficient spectral resolution. We call this effect resolution-linked bias (hereafter, RLB). Sec. 2 describes the source of RLB, and Sec. 3 evaluates its magnitude for the recent case of the TRAPPIST-1b exoplanet. Sec. 4 concludes with some remarks on the future importance of the RLB effect.

2. SOURCE OF RESOLUTION-LINKED BIAS

We begin here by reminding the reader of the spectral resolving power needed to resolve intrinsic line widths in stellar and planetary spectra (Sec. 2.1). We then explain the source of RLB using a simple numerical example (Sec. 2.2) and physical arguments, and then with a general mathematical formalism (Sec. 2.3).

2.1. Resolving Stellar and Exoplanetary Spectra

Two principal mechanisms broaden lines in stellar and planetary spectra: Doppler broadening and pressure broadening. The physical principles of spectral line broadening are already well understood (Rybicki and Lightman 1979), but we apply these principles to the TRAPPIST-1 system in order to provide a context for our discussion of RLB.

The Doppler width of a spectral line is determined by the line-of-sight thermal motion of the absorbing species, being proportional to the square root of temperature ($\Delta\nu = \nu_0/c\sqrt{(2kT/m)}$), where k is Boltzmann's constant and m is the mass of the absorbing atom or molecule). Table 1 summarizes the Doppler and pressure-broadened widths for 1.4 μm water vapor absorption in the continuum and line-forming regions of the stellar and planetary atmospheres in the TRAPPIST-1b system. We adopted pressures and temperatures for these regions based on the $T_{\text{eff}}/\log g/[M/H] = 2500/5.5/0.0$ Phoenix stellar model

¹ Department of Astronomy, University of Maryland at College Park, College Park, MD 20742, USA

² NASA Astrobiology Institute's Virtual Planetary Laboratory

(Husser et al. 2013), and an isothermal atmosphere for the planet at the estimated equilibrium temperature of 400K (Gillon et al. 2017). The exact pressures and temperatures are not critical to the main point of Table 1: nearly all stellar and exoplanetary observed spectra fail to resolve the widths of individual spectral lines. The requisite spectral resolving powers ($\nu/\Delta\nu$) range from over 10^5 for the continuum-forming regions of the stellar atmosphere, to over 10^7 for low pressure regions of the exoplanetary atmosphere.

No current or planned space-borne spectrometer can attain the spectral resolving powers listed in Table 1. Grism spectroscopy with HST/WFC3 at $1.4\mu\text{m}$ achieves a resolving power of about 130 (and usually less because of binning), which is several orders of magnitude less than required to resolve individual spectral lines of water vapor. The situation is similar for JWST, where near- and mid-IR resolving powers will range from 700 (NIRISS) to 2700 (NIRSpec). We do not make this comparison as a criticism of these instruments: low to moderate spectral resolving power is necessary in order to attain adequate signal-to-noise for many measurements. Rather, we emphasize that the observed spectra do not come even close to resolving the intrinsic line widths.

Figure 1 shows an example of an M-dwarf spectrum, from the Phoenix model (Husser et al. 2013) appropriate for the host star in TRAPPIST-1. The spectrum at a resolving power ($\lambda/\delta\lambda$) of 5.0×10^5 is a forest of line-resolved structure (in gray on top panel). We convolved that spectrum with a Gaussian instrument profile, to a spectral resolving power of 1000 (blue spectrum in the top panel). At that resolving power, water absorption remains prominent in the spectrum, but the depths of the bands appear modest. However, at full resolution the individual absorption lines due to water vapor are very strong: many have core intensities below 0.1 of the local continuum level. Note also that these ‘lines’ are not individual quantum transitions. Between 7000 and 9000 cm^{-1} there are about 50 million discrete transitions in the line list from Barber et al. (2006). What appear to be single lines on Figure 1 are actually composed of (in most cases) hundreds of distinct quantum transitions. However, the wavelength scale of structure in the spectrum is still dictated by the broadening mechanisms discussed above.

In addition to line broadening, relative wavelength shifts of lines in the star versus a transiting planet are relevant to RLB. Many transiting planets have circular orbits, providing only minimal Doppler shifts between the stellar and planetary lines during transit (e.g., from stellar rotation, and the projection of the planet’s orbital velocity onto the stellar disk). Line overlap due to small relative Doppler shifts tend to maximize RLB (Sec. 3). TRAPPIST-1 is a rapid rotator (P=1.4d, Gillon et al. 2016), with an equatorial rotation speed of 4.2 km/sec. The planet’s orbital velocity is 80 km/sec, and the component projected onto the stellar disk during transit is ≤ 4 km/sec, and that tends to reduce the relative radial velocity difference, assuming that the planet orbits in the same direction as stellar rotation. A significant RLB effect results from the velocity difference, as we show in Sec. 3.

Stellar granular convection is another source of Doppler shifts. IR lines in M-dwarf spectra are not well stud-

ied in terms of convective Doppler shifts, but hydrodynamic simulations indicate granular convective velocities of ~ 240 meters/sec (Ludwig et al. 2002), too small to be significant in this context.

Winds in hot exoplanet atmospheres can produce Doppler shifts of planetary lines by several km/sec (Kempton et al. 2014), but a velocity of that magnitude will still leave substantial overlap between the stellar and planetary lines.

The mechanisms discussed above do not shift exoplanetary spectral lines enough to prevent substantial overlap with stellar lines, and the overlap is the source of RLB.

2.2. A Simple Numerical Example

We begin our explanation of RLB with a simple numerical example. Consider wavelengths λ_1 and λ_2 , and out-of-transit stellar fluxes F_1 and F_2 . The fine-scale spectral structure seen in Figure 1 can lead to a significant difference between F_1 and F_2 , so (for example) we might have $F_2 = 0.1F_1$ if λ_2 is centered on a water vapor line in both the planet and star - which is possible because of the small relative Doppler shift as noted above. We let the area (i.e., solid angle) of the planet (in units of the stellar disk area) at wavelength λ_1 be A , and let the absorbing atmospheric annulus have area δ , only at wavelength λ_2 .

Now consider the depth of the transit, by comparing stellar fluxes in transit and out of transit. At wavelength λ_2 where the exoplanetary atmosphere is strongly absorbing, the in transit flux is $0.1F_1(1 - A - \delta)$, so the depth of the transit being (out-in)/out, is:

$$(0.1F_1 - 0.1F_1(1 - A - \delta))/0.1F_1 = A + \delta \quad (1)$$

and similarly at λ_1 , the depth of the transit is A . As long as λ_1 and λ_2 are spectrally resolved, there is no RLB effect. However, as we noted in Sec. 2.1, fine scale structure in M-dwarf spectra is often unresolved and observations can only sense the total flux in a resolution element. So the observed transit depth becomes:

$$(1.1F_1 - (F_1(1 - A) + 0.1F_1(1 - A - \delta)))/1.1F_1 = A + 0.091\delta \quad (2)$$

The transit light curve at λ_2 is diluted by the greater stellar flux at λ_1 , where neither the planet nor star has water vapor absorption. Therefore the transit at the observed spectral resolving power can in principle exhibit a much lower apparent absorption than actually occurs in the monochromatic spectrum.

In this example, the RLB effect would be absent if the two wavelengths were spectrally resolved, because the ratio of in-transit to out-of-transit flux is accurate at each wavelength. However, when the wavelengths are averaged by low spectral resolving power, then the ratio of the average fluxes does not preserve the spectral transmission information accurately. Fundamentally that derives from the nonlinearity of ratios: a ratio of averages is not equal to an average of ratios.

Physically, we can envision a case where water absorption in the exoplanetary atmosphere occurs in a series of discrete lines that are centered on stellar water absorption lines. At the water wavelengths the star is much fainter than in the continuum, so the water absorption

during transit is readily overwhelmed by flux at wavelengths where no water absorption occurs. In a real situation, important additional factors include the relative strengths of water lines in the planet and star due to their different excitation temperatures, different line broadening, and the stellar rotational velocity. For example, if the planetary lines were much broader than the stellar lines, or the planet’s orbital velocity was large and retrograde, then the RLB effect will be correspondingly reduced by the mismatch in line profiles or wavelengths. We include all relevant effects in our calculations of Sec. 3.

2.3. Mathematical Formalism

We here give a more formal mathematical description of RLB. Let the monochromatic flux of the star at wavelength λ be F_λ , and let the absorption of the exoplanetary atmosphere at λ be A_λ ($1 - A_\lambda$ is transmitted). We observe the spectrum with less than line-resolved resolution, and we denote the spectral instrumental profile as I_λ . The measured spectrum during a transit is of the form $(out - in)/out$ where *in* and *out* refer to the measured flux in and out of transit. In that form, the measured signal S_λ is:

$$S_\lambda = \frac{I_\lambda \otimes F_\lambda - I_\lambda \otimes (F_\lambda(1 - A_\lambda))}{I_\lambda \otimes F_\lambda}, \quad (3)$$

$$= 1 - \frac{I_\lambda \otimes (F_\lambda(1 - A_\lambda))}{I_\lambda \otimes F_\lambda}, \quad (4)$$

where \otimes denotes convolution. Instead of Eq.(4), a more usual practice is to represent the star out of transit using a low resolution spectrum F'_λ , and to write the in transit flux as $F'_\lambda(1 - A_\lambda)$. In that case, the stellar flux cancels in the $(out - in)/out$ expression, and $S_\lambda = A_\lambda$. But since A_λ is often modeled at a spectral resolution higher than the observations, the result is convolved with I_λ in an *ad hoc* fashion, i.e.;

$$S_\lambda = I_\lambda \otimes A_\lambda \quad (5)$$

The necessity for doing a convolution to the observed resolution in an *ad hoc* fashion is a clue that Eq.(5) is not strictly correct. In Sec. 3, we illustrate the difference between the approximation represented by Eq.(5) and the strictly correct Eq.(4); the magnitude of that difference is the RLB effect.

3. MAGNITUDE OF RESOLUTION-LINKED BIAS FOR A REPRESENTATIVE CASE

We here calculate the RLB effect for the exoplanet TRAPPIST-1b (de Wit et al. 2016). We choose this system as an example because the host star is a late M-dwarf, and its spectrum is rich in molecular absorption lines, potentially producing a significant RLB effect. Sec. 3.1 describes the radiative transfer aspect of our calculations, Sec. 3.2 explains our treatment of line opacity, and Sec. 3.3 describes how we tested our codes. Sec. 3.4 shows the magnitude of the RLB effect for TRAPPIST-1b.

3.1. Exoplanetary and Stellar Model Spectra

We model the star using a $T_{\text{eff}}/\log g/[M/H] = 2500/5.5/0.0$ Phoenix stellar model (Husser et al. 2013), and we use an isothermal atmosphere at 400K for the planet (as in Sec. 2.1). We derive our water absorption line opacities for both the planet and star using the line list from Barber et al. (2006). Our transit spectrum of the TRAPPIST-1b planet is calculated by the code described by Deming et al. (2013); our stellar spectral code is new to this paper. We produce both the flux and intensity spectrum of the TRAPPIST-1 star, based on the pressure-temperature relation of Phoenix model cited above. Because the planet is smaller than the stellar disk, disk-resolved intensity (not flux) calculations are appropriate for modeling the RLB effect. However, the Phoenix models tabulate emergent flux, so it is convenient to check our code versus the Phoenix flux spectrum. We adopt the pressure-temperature relation, and the solar composition and $\log(g) = 5.5$, of the Phoenix model. Our continuous opacity is due to H_2 Rayleigh scattering (Dalgarno & Williams 1962), as well as H_2 collision-induced opacity (Zheng & Borysow 1995; Borysow 2002). For both the planet and star, our line opacity uses only water vapor. We calculate the emergent intensity using a high-resolution wavelength grid (0.4 km sec⁻¹ spacing). At each wavelength, we interpolate the optical depths in the model to a uniform grid in $\log(\tau)$ to facilitate accurate integration. Adopting an LTE source function, we calculate emergent intensity from the formal solution of the transfer equation (Rybicki and Lightman 1979), integrating on the uniform grid using Laguerre polynomial weights. We derive the flux spectrum using an 8-point Gaussian quadrature integration over intensity as a function of emergent angle.

3.2. Line Opacity Calculations

The water vapor line list from Barber et al. (2006) is too extensive to treat each line with an individual Voigt profile. As advocated by Grimm & Heng (2015), we here describe exactly how we calculate line opacity. Our method is based on the fact that many line centers overlap within each Doppler width, so we average those lines to form a single equivalent ‘pseudo-line’. We adopt a grid of equally spaced frequencies (this is different than the grid used to calculate the spectra). Within each grid interval we add the strengths of all lines whose central rest frequency falls in the interval to form a single pseudo-line per interval. Because the lines have different lower state excitation energies, the sum of their strengths is temperature-dependent. We tabulate the summed strength at 10 temperatures spanning the range in the models, and we fit the results to within 2% in line strength using a 4th order polynomial as a function of temperature. This pre-processing produces a list of pseudo-lines spaced at 0.005 cm⁻¹ intervals, and reduces the number of lines by a factor of ~ 100 from the original Barber et al. (2006) list. We use a pressure broadening coefficient of 0.06 cm⁻¹ per atmosphere for all lines. Husser et al. (2013) infer negligibly small microturbulence for TRAPPIST-1, so we ignore microturbulence except for one exploratory calculation mentioned in Sec. 3.4.

3.3. Tests of the Calculations

To ensure accurate evaluation of the RLB effect, we tested the precision and accuracy of our calculations. Our planetary transmittance code was previously checked against independent calculations from Fortney et al. (2010) (see Figure 12 of the Deming et al. 2013 paper). The same code was also compared to a second independent calculation by Line et al. (2013). In our stellar calculations, we verified adequate precision of the integrations by setting the atmospheric temperature to be isothermal, and comparing the calculated intensity and flux to the analytic Planck function at that temperature (an LTE isothermal atmosphere emits as a blackbody). We found that the emergent intensities were accurate to 0.1%, and the flux was accurate to 1.1%. (Note that we do not require accuracy of the intensities and fluxes in an absolute sense, we only require that the relative shape of emergent spectral lines be correct.) Finally, we tested our flux calculation by comparison to the high resolution Phoenix flux from Husser et al. (2013). That comparison is shown for an expanded region near the $1.4\ \mu\text{m}$ water band in Figure 2. Overall, we find excellent agreement, with our spectrum showing more absorption in some regions. Those differences are as expected, because the Phoenix line opacity uses a line strength cutoff (P. Hauschildt, private communication), whereas we include all of the lines from Barber et al. (2006). We conclude that our calculations are accurate, and - most important - they are self-consistent from planet to star.

We tested our line averaging procedure by varying the size of the grid interval used for the averaging. In the limit where the interval approaches zero, our averaging reduces to a true line-by-line calculation. We verified that the spectrum approaches that limit as we reduced the interval. We found that interval widths less than $0.01\ \text{cm}^{-1}$ produced negligible differences from a line-by-line calculation, but to be conservative we used a $0.005\ \text{cm}^{-1}$ grid for our models.

3.4. Magnitude of the Effect for TRAPPIST-1b

We calculated a transmission spectrum for TRAPPIST-1b, adopting an isothermal solar composition atmosphere at $T=400\text{K}$. In order to explore the potential temperature dependence of RLB, we also calculated for an exoplanetary temperature of 800K (although the planet is not sufficiently irradiated to be that hot). We did an exact calculation using Eq. (4), and also the conventional (i.e., approximate) calculation using Eq. (5). In all cases we used the pressure-temperature relation of the Phoenix model to calculate emergent intensity spectra, as described in Sec. 3. We multiplied each intensity spectrum times the planetary transmittance, and averaged over 11 points equally spaced across the stellar disk during transit. In the exact calculation, we accounted for the stellar rotation, the projection of the planet's orbital velocity, and the gravitational redshift when multiplying the stellar spectra times the transmittance of the exoplanetary atmosphere.

Figure 3 shows the results of our calculations. The transit spectrum of a solar composition atmosphere for

TRAPPIST-1b in this HST/WFC3 bandpass has an amplitude of about 2000 ppm (as already shown by de Wit et al. 2016). The difference between the exact and approximate calculation represents the RLB effect. RLB is significant in the strongest portion of the band between 1.35 and $1.4\ \mu\text{m}$. The difference (plotted on the lower portion of Figure 3) is about 250 ppm, 12% of the peak transmittance. For the 800K atmosphere, the RLB effect is about 900 ppm, almost four times as large as for the 400K atmosphere. A factor of two is due to the greater scale height of the 800K atmosphere, but a comparable factor comes from the excitation structure of the water band, wherein the higher planetary temperature increases the match between the stellar and exoplanetary spectrum. We also tested the effect of a possible $2\ \text{km/sec}$ stellar microturbulence, and we find that it decreases the RLB effect only slightly (35 ppm).

4. CONCLUDING REMARKS

The RLB effect for TRAPPIST-1b is not sufficient to alter the conclusions of the study by de Wit et al. (2016). Interestingly, the effect is about the same amplitude as the *total* absorption due to water vapor in a typical hot Jupiter (e.g., Deming et al. 2013). As for hot Jupiters, most of them transit FGK stars, where the RLB effect due to water vapor will be negligible.

Although RLB is not a major factor affecting current observations, it will be important to include it when modeling future JWST observations, especially of super-Earths and mini-Neptunes transiting M-dwarfs. TESS will discover many such worlds that are favorable for observations using JWST. Based on our exploratory calculations to date, we expect that RLB will be strongest for hot planets in prograde orbits around M-dwarf host stars, although it will be reduced for cases where the planet's orbital velocity is very high. The molecular bands in the JWST spectral range tend to be intrinsically stronger than in the HST/WFC3 band, and that should also lead to a larger RLB effect. Given anticipated high signal-to-noise from JWST transit spectroscopy, it is likely that RLB will be well above the observational precision in many cases. Because RLB affects the strongest portions of molecular bands, ignoring it would cause systematic errors in atmospheric retrievals at the highest altitudes. Although it is primarily of concern for M-dwarf host stars, stars as hot as the Sun can have significant absorption in the fundamental carbon monoxide band near $4.6\ \mu\text{m}$ (Uitenbroek et al. 1994). Hence JWST spectroscopy of planets transiting GKM stars should be evaluated for significant RLB effect on carbon monoxide retrievals.

We thank an anonymous referee for insightful and constructive comments that improved this paper, and we acknowledge informative correspondence with the Phoenix group, specifically Tim-Oliver Husser, Ansgar Reiners, and Peter Hauschildt. We also gratefully acknowledge NASA grant NNX15AE19G, and support from NASA's Virtual Planetary Laboratory.

REFERENCES

- Anglada-Escude, G., et al., 2016, *Nature*, 536, 437
 Barber, R. J., Tennyson, J., Harris, G. J., and Tolchenov, R. N. 2006, *MNRAS*, 368, 1087
 Barstow, J. K., & Irwin, P. G. J. 2016, *MNRAS*, 461, L92.
 Beichman, C., et al., 2014, *PASP*, 126, 1134
 Berta-Thompson, Z. K., et al., 2015, *Nature*, 527, 204
 Borysow, A., 2002, *A&A*, 390, 779.
 Brown, T. M., 2001, *ApJ*, 553, 1006
 Charbonneau, D., Brown, T. M., Noyes, R. W., and Gilliland, R. L., 2002, *ApJ*, 568, 377
 Cowan, N. B., et al. 2015, *PASP*, 127, 311
 Dalgarno, A. & Williams, D. A. 1962, *ApJ*, 136, 690
 Deming, D., et al., 2009, *PASP*, 121, 952
 Deming, D., et al., 2013, *ApJ*, 774, id.95
 de Wit, J., et al., 2016, *Nature*, 537, 69.
 Dravins, D. 1987, *A&A*, 172, 211
 Evans, T. M., et al., 2016, *ApJ*, 822, id.L4
 Fortney, J. J., Shabram, M., Showman, A. P., Lian, Y., Freedman, R. S., Marley, M. S., & Lewis, N. K., 2010, *ApJ*, 709, 1396
 Fraine, J., Deming, D., Benneke, B., Knutson, H., Jordan, A., Espinoza, N., Madhusudhan, N., Wilkins, A., & Todorov, K., 2014, *Nature*, 513, 526
 Gillon, M., et al., 2016, *Nature*, 533, 221
 Gillon, M., et al., 2017, *Nature*, 542, 456
 Greene, T. R., Line, M. R., Montero, C., Fortney, J. J., Lustig-Yaeger, J., and Luther, K., 2016, *ApJ*, 817, id.17
 Grimm, S. L., & Heng, K. 2015, *ApJ*, 808, id.182
 Heng, K., Lyons, J. R., & Shang-Min, T. 2016, *ApJ*, 816, id.96
 Hubbard, W. B., Fortney, J. J., Lunine, J. I., Burrows, A., Sudarsky, D., and Pinto, P., 2001, *ApJ*, 560, 413
 Husser, T. O., Wende-von Berg, S., Dreizler S., Homeier, D., Reiners, A., Barman, T., and Hauschildt, P. H. 2013, *A&A*, 553, id.A6
 Knutson, H. A., et al., *ApJ*, 794, id.155
 Kempton, E. M.-R., Perna, R., & Heng, K. 2014, *ApJ*, 795, id.24
 Kreidberg, L., et al., 2014a, *ApJ*, 793, id.L27
 Kreidberg, L., et al., 2014b, *Nature*, 505, 69
 Line, M. R., Knutson, H., Deming, D., Wilkins, A., & Desert, J.-M. 2013, *ApJ*, 778, id.183
 Ludwig, H. G., Allard, F., and Hauschildt, P. H. 2002, *A&A*, 395, 99
 Newton, E., Irwin, J., Charbonneau, D., Berlind, P., Calkins, M. L., & Mink, J. 2016, *ApJ*, 834, id.85.
 Nikolov, N., et al., 2015, *MNRAS*, 447, 463
 Partridge, H., & Schwenke, D. W., 1997, *J. Chem. Phys.*, 106, 4618.
 Redfield, S., Endl, M., Cochran, W. D., and Koesterke, L., 2008, *ApJ*, 673, id.L87
 Ricker, G., et al., 2015, *JATIS*, 1, id.014003
 Rybicki, G. B., and Lightman, A. P., 1979, *Radiative Processes in Astrophysics*, New York: John Wiley & Sons
 Sing, D. K., et al., 2016, *Nature*, 529, 59
 Stevenson, K., et al., 2016, *PASP*, 128, 967
 Uitenbroek, H., Noyes, R. W., & Rabin, D. 1994, *ApJ*, 432, L67
 Zheng, C., & Borysow, A., 1995, *ApJ*, 411, 960.

TABLE 1
 DOPPLER WIDTH, AND PRESSURE-BROADENED WIDTHS (IN cm^{-1}) FOR WATER VAPOR LINES NEAR $1.4 \mu\text{M}$ IN THE ATMOSPHERES
 OF THE STAR AND PLANET 'B' IN THE TRAPPIST-1 SYSTEM.

Atmospheric level	Temperature or Pressure	$\Delta\nu$	$\nu/\Delta\nu$
Star, continuum	2760 K	0.038	1.89×10^5
Star, continuum	1.75 bar	0.105	6.80×10^4
Star, line region	1700 K	0.030	2.40×10^5
Star, line region	80 mbar	0.0048	1.50×10^6
Planet, troposphere	400 K	0.014	4.95×10^5
Planet, troposphere	1 bar	0.060	1.19×10^5
Planet, upper atmosphere	10 mbar	0.0006	1.19×10^7

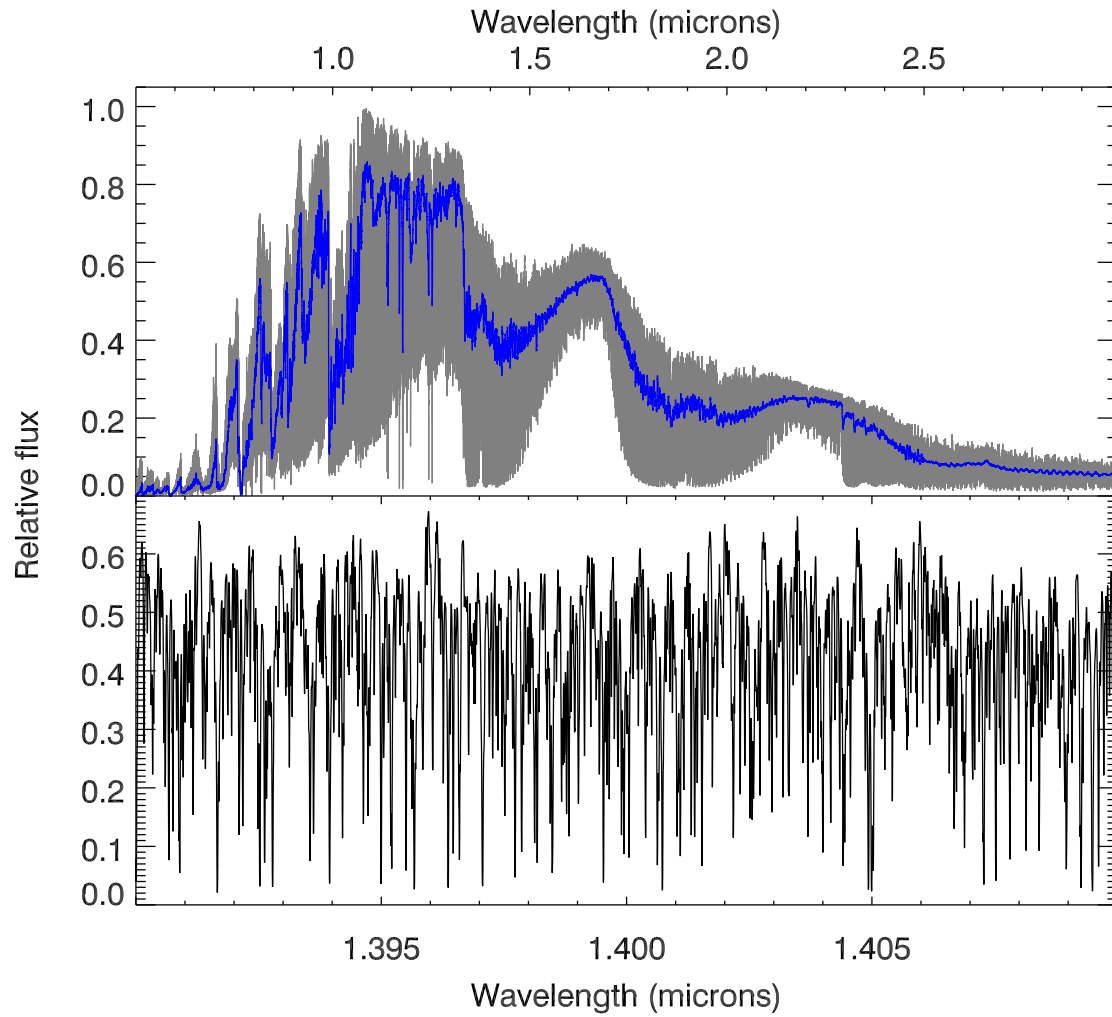


FIG. 1.— Near-infrared flux from a Phoenix model atmosphere with $T_{\text{eff}}/\log g/[Fe/H]$ of 2500/5.5/0.0 from Husser et al. (2013). The top panel plots the spectrum at full resolution in gray, and convolved to a spectral resolving power of 1000 (blue). The lower panel expands a small section of the spectrum near $1.4\mu\text{m}$. Note the deep and abundant absorption lines.

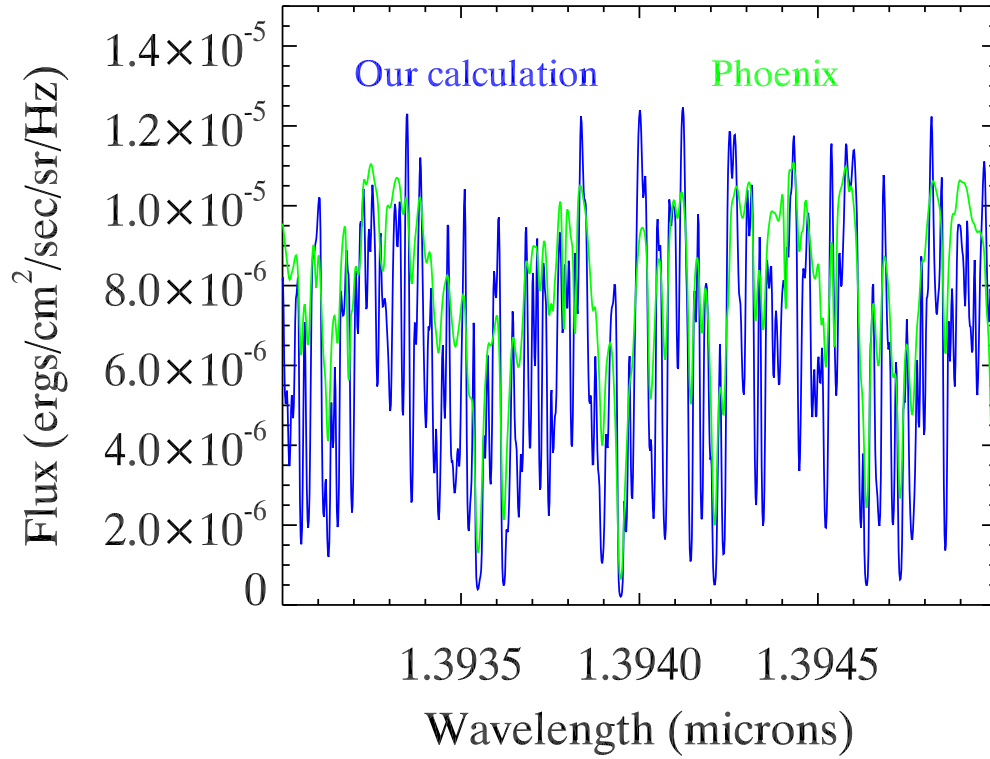


FIG. 2.— For an expanded wavelength region near the 1.4 μm water vapor band head, we here test our calculated stellar flux (blue line) by comparing to the flux from Husser et al. 2013 (green line). We use the temperature/pressure relation of the Phoenix model atmosphere with $T_{\text{eff}}/\log g/[\text{Fe}/\text{H}]$ of 2500/5.5/0.0.

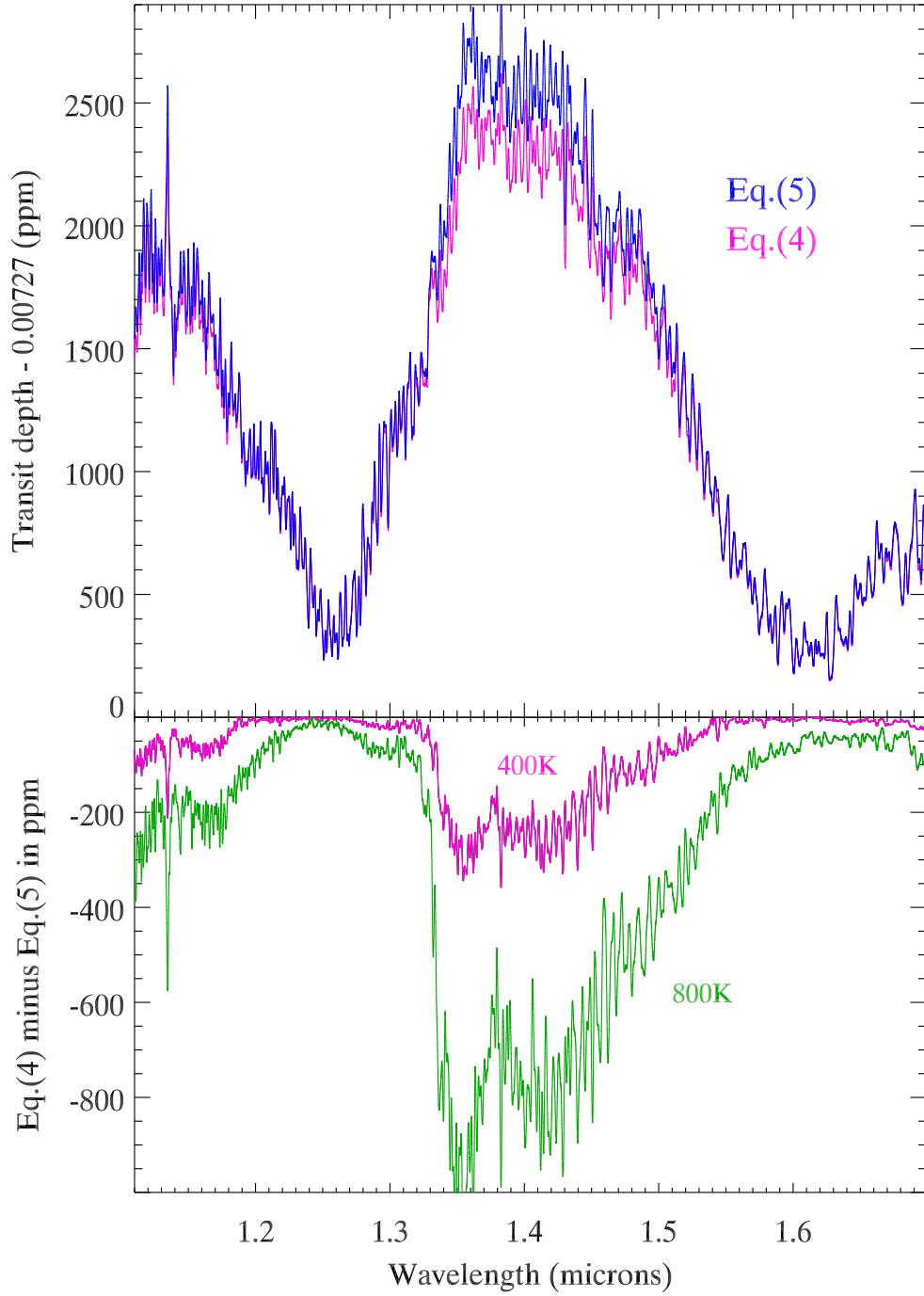


FIG. 3.— Top panel: transmission spectrum of TRAPPIST-1b modeled with the exact relation (Eq. 4) versus the approximate method that is commonly used (Eq. 5). Bottom panel: the difference between Eq. 4 and Eq. 5 for our nominal model with an exoplanetary atmospheric temperature of 400K. Also plotted is the difference if the exoplanetary temperature were 800K.